Electron impact excitation of n=3 states of C III: an application of a new R-matrix package

To cite this article: K A Berrington *et al* 1989 *J. Phys. B: At. Mol. Opt. Phys.* **22** 665

View the article online for updates and enhancements.

Related content

- Electron impact excitation of C III in a twelve-state R-matrix calculation. Effective collision strengths between the n=2 states
  K A Berrington

- Collision strengths for the electron impact excitation of Ca XIII
  K S Baliyan and A K Bhatia

- Use of the Burgess sum rule in calculating cross sections for electron impact excitation of optically allowed transitions in positive ions
  V M Burke and M J Seaton

Recent citations

- Hot prominence detected in the core of a coronal mass ejection
  S. Jeji *et al*

- Energy levels, radiative rates and electron impact excitation rates for transitions in C iii
  Kanti M. Aggarwal and Francis P. Keenan

- Contribution to the theoretical investigation of electron and photon interaction with carbon atom and its ions
  V Stancalie

Electron impact excitation of $n = 3$ states of C III: an application of a new R-matrix package

K A Berrington, V M Burke, P G Burke and S Scialla†

Department of Applied Mathematics and Theoretical Physics, The Queen's University of Belfast, Belfast BT7 1NN, UK

Abstract. The R-matrix method is used to obtain effective collision strengths for the beryllium-like ion C III for all transitions between the six $n = 2$ states with configurations $2s^2$, $2s2p$ and $2p^2$ and the six $n = 3$ states with configurations $2s3s$, $2s3p$ and $2s3d$. In addition effective collision strengths between all pairs of these $n = 3$ states are calculated. The calculations are carried out including the first twelve target eigenstates in the R-matrix expansion of the total wavefunction. In order to obtain converged cross sections involving the $n = 3$ states a new no-exchange R-matrix package was developed and is described in this paper. This package, combined with the Burgess sum rule, is used to determine the high partial wave contributions to the cross section. Results for the effective collision strengths are presented in tabular form for temperatures in the range 10^4–$10^{5.8}$ K.

1. Introduction

Transitions amongst terms of the $n = 2$ and $n = 3$ configurations in the beryllium-like ion C III are observed in a wide variety of astronomical objects and laboratory plasmas (e.g., Gabriel and Jordan 1972, Dufton and Kingston 1981). In order to interpret the observational results it is necessary to have reliable atomic data for both the radiative and electron collisional rates for these transitions. The present paper is a continuation of a programme of research initiated by Burke *et al* (1972) to determine such data for all ions of the beryllium isoelectronic sequence.

In most of the earlier work on C III, the six lowest states arising from the $2s^2$, $2s2p$ and $2p^2$ configurations were included in the R-matrix expansion of the total wavefunction. Collision strengths from these calculations obtained by Berrington *et al* (1977, 1981, 1985) have been used in the calculation of level populations for astrophysical plasmas (Keenan *et al* 1984) emission line ratios in the sun (Dufton *et al* 1978) and solar opacities (Doyle and McWhirter 1980). In addition, this same six-state approximation has recently been used as the basis of calculations of C II oscillator strengths (Yu Yan *et al* 1987), C II photoionisation cross sections (Yu Yan and Seaton 1987a, b) and C III electron impact line broadening (Seaton 1989) which form part of a general study of stellar opacities.

Recently, in addition to the six lowest states of C III, the six states arising from the configurations $2s3s$, $2s3p$ and $2s3d$ have been included in a 12-state R-matrix expansion of the total wavefunction. The purpose of this new work is firstly to determine the

---

† On leave of absence from Departmento di Chimica, Citta Universitaria, Rome, Italy.

effect of the 2s3*l* states on the earlier six-state calculations and secondly to calculate electron collision strengths involving the 2s3*l* states. The first of these aims was the basis of an earlier paper by Berrington (1985). The purpose of the present paper is to present results which accomplish the second objective. This work will enable observations of allowed and forbidden transitions between the $n = 3$ complex of levels and the $n = 2$ complex of levels to be interpreted for the first time.

An important aspect of our present work involving excitation of the $n = 3$ levels is the slow convergence of the partial wave expansion of the cross section. Indeed, at the highest energies considered in this paper, partial wave contributions up to total angular momentum $L \approx 35$ had to be included before the sum rule of Burgess (1974) could be used. If we had used the standard R-matrix package (Berrington *et al* 1974, 1978) for all of these partial waves the computer time involved would have been excessive. We have therefore developed a new no-exchange R-matrix package which gave accurate results for the transitions considered here for all $L \geq 11$. This enabled considerable time to be saved since for this work it ran about 50 times faster than the standard R-matrix package. This new package is written generally so that it will calculate no-exchange cross sections for any atom or ion and is now being used in our work on many other systems.

The rest of the paper is organised as follows. In § 2 we describe the approximation which we have used. We give tables of the orbital coefficients and the excitation thresholds and we describe the expansions of the target states and of the collision states. In § 3 we describe our new no-exchange R-matrix package. The no-exchange package itself will be published elsewhere (Burke and Burke 1989). In § 4 we describe how we have combined the results from this new package with the Burgess sum rule to obtain converged cross sections. In § 5 we describe our results and give tables of effective collision strengths both for the $n = 2$ to $n = 3$ transitions and for the $n = 3$ to $n = 3$ transitions. Finally, in § 6 we draw some conclusions from our work and describe future directions of research.

2. The approximation

2.1. The target states

We have included the 2s^2 ^{1}S^e; 2s2p ^{3}P^o, ^{1}P^o; 2p^2 ^{3}P^e, ^{1}D^e, ^{1}S^e; 2s3s ^{3}S^e, ^{1}S^e; 2s3p ^{3}P^o, ^{1}P^o and 2s3d ^{3}D^e, ^{1}D^e target states in our calculation. These are represented in terms of ten orthonormal basis orbitals and pseudo-orbitals 1s, 2s, 2p, 3s, 3p, 3d, $\overline{4s}$, $\overline{4p}$, $\overline{4d}$ and $\overline{4f}$ calculated by Hibbert (1976). Each of these orbitals is expanded in the form

$$P_{nl}(r) = \sum_i c_i r^{p_i} \exp(-\xi_i r) \tag{1}$$

where the coefficients c_i, p_i and ξ_i are given in table 1.

The target states Φ_i are expanded as linear combinations of configurations φ_i

$$\Phi_i(1, \ldots, N) = \sum_{i'} \varphi_{i'}(1, \ldots, N) c_{i'i} \tag{2}$$

where the program CIV3 written by Hibbert (1975) was used both to optimise the coefficients defining the orbitals in equation (1) and to determine the coefficients $c_{i'i}$ in equation (2). The basis configurations φ_i were generated automatically by requiring that two of the target electrons are retained in the 1s shell and the other two electrons (remembering that the number of target electrons N in equation (2) is four for C III)

Table 1. Coefficients for the atomic orbitals defined by equation (1). The power of ten multiplying the number is given after the comma.

	c_i	p_i	ξ_i		c_i	p_i	ξ_i
1s	0.227 69, 2	1	0.529 12, 1	2p	0.348 16, 0	2	0.249 81, 1
	0.495 17, 1	1	0.912 78, 1		0.175 78, 1	2	0.387 00, 1
	0.100 82, 0	2	0.202 90, 1		0.500 72, 1	2	0.185 00, 1
	−0.129 31, 1	2	0.468 91, 1		0.109 93, 1	2	0.825 00, 1
	−0.525 80, −1	2	0.175 38, 1	3p	−0.242 05, 1	2	0.357 00, 1
2s	−0.502 23, 1	1	0.950 00, 1		−0.793 81, −1	3	0.357 00, 1
	−0.885 23, 1	2	0.950 00, 1		−0.238 08, 1	4	0.357 00, 1
	−0.119 81, 1	1	0.540 00, 1		−0.157 05, 1	2	0.109 00, 1
	−0.133 13, 2	2	0.540 00, 1		0.109 63, 1	3	0.109 00, 1
	−0.119 95, 1	1	0.215 00, 1		−0.768 01, −2	4	0.109 00, 1
	−0.968 67, 1	2	0.215 00, 1	$\overline{4p}$	0.499 35, 1	2	0.111 85, 1
3s	0.507 30, 1	1	0.465 00, 1		−0.493 25, 1	3	0.111 85, 1
	0.347 81, 1	2	0.465 00, 1		0.960 89, 0	4	0.111 85, 1
	0.762 87, 1	3	0.465 00, 1	3d	−0.260 74, 0	3	0.200 00, 1
	−0.193 30, 1	1	0.119 00, 1		−0.357 00, −2	4	0.200 00, 1
	−0.969 69, 0	2	0.119 00, 1		−0.453 44, 0	3	0.103 00, 1
	0.134 69, 1	3	0.119 00, 1		0.128 00, −2	4	0.103 00, 1
$\overline{4s}$	0.751 17, 1	1	0.530 00, 1				
	−0.909 94, 1	2	0.200 00, 1	$\overline{4d}$	0.111 57, 2	3	0.191 41, 1
	0.367 38, 1	3	0.120 00, 1		−0.478 43, 1	4	0.191 41, 1
	0.367 38, 1	3	0.120 00, 1				
	−0.101 55, 1	4	0.120 00, 1	$\overline{4f}$	0.705 04, 0	4	0.150 30, 1

are distributed amongst the other nine shells in all possible ways with the restriction that not more than one electron is allowed in the $\overline{4f}$ shell. In this way, the number of configurations generated was 15 for $^1S^e$ symmetry, 7 for $^3S^e$ symmetry, 17 for $^1P^o$ symmetry, 26 for $^3P^o$ symmetry, 18 for $^1D^e$ symmetry and 13 for $^3D^e$ symmetry. We compare our calculated excitation thresholds with observations in table 2. We see that

Table 2. Calculated excitation thresholds in Rydbergs compared with observed values given by Moore (1970).

	Calculated	Observed
$2s^2\ ^1S^e$	0.0	0.0
$2s2p\ ^3P^o$	0.4776	0.4776
$2s2p\ ^1P^o$	0.9575	0.9327
$2p^2\ ^3P^e$	1.2610	1.2528
$2p^2\ ^1D^e$	1.3482	1.3293
$2p^2\ ^1S^e$	1.6986	1.6633
$2s3s\ ^3S^e$	2.1612	2.171
$2s3s\ ^1S^e$	2.2462	2.252
$2s2p\ ^1P^o$	2.3531	2.360
$2s2p\ ^3P^o$	2.3591	2.367
$2s3d\ ^3D^e$	2.4506	2.461
$2s3d\ ^1D^e$	2.5179	2.519

the agreement is very satisfactory. Nevertheless, in order to make an exact comparison with experiment we have adopted the observed excitation thresholds in our collision calculations. Further information on these target states and on the calculated transition oscillator strengths are given by Hibbert (1976) and by Glass (1979).

2.2. The collision wavefunction

The total wavefunction describing the collision is expanded in the R-matrix internal region in terms of the following basis

$$\psi_k = \mathscr{A} \sum_{ij} \bar{\Phi}_i(1, \ldots, N; \hat{r}_{N+1}\sigma_{N+1})r_{N+1}^{-1}u_j(r_{N+1})a_{ijk} + \sum_j \chi_j(1, \ldots, N+1)b_{jk}. \tag{3}$$

The $\bar{\Phi}_i$ are channel functions formed by coupling the target states to the spin-angle function of the scattered electron as described in the next section, the u_j are continuum basis functions representing the scattered electron and the χ_j are quadratically integrable functions constructed from the ten bound orbitals. $\mathscr{A}$ is the antisymmetrisation operator which ensures that the total wavefunction satisfies the Pauli exclusion principle.

The u_j are chosen to satisfy a zero-order differential equation subject to the boundary conditions

$$u_j(0) = 0 \qquad \frac{a}{u_j} \frac{\mathrm{d}u_j}{\mathrm{d}r}\bigg|_{r=a} = 0 \tag{4}$$

where $a = 14$ au is the radius of the internal region. They are orthonormal and orthogonal to the bound orbitals over this interval. In practice about 19 continuum basis functions are retained in each channel which is sufficient to give convergence for all energies and angular momenta considered. The χ_j are constructed automatically by requiring that two electrons are retained in the 1s shell and the other three electrons are distributed amongst the other nine shells in all possible ways with the restriction that not more than two electrons are allowed in the $\overline{4f}$ shell. Further details concerning expansion (3) have been given by Burke and Robb (1975) and Berrington *et al* (1974, 1978).

3. A new no-exchange *R*-matrix package

In order to obtain converged cross sections for transitions between the $n = 3$ target states, the calculation had to be carried out for a large number of partial waves. The low partial waves were calculated using the standard R-matrix package of Berrington *et al* (1974, 1978). However it proved inefficient to use this package for the many high partial waves where electron exchange effects are negligible but where strong channel coupling effects are still important. A new no-exchange R-matrix package was therefore developed which enabled the high partial wave cross sections to be determined very rapidly. The theory of the no-exchange calculations is described below. For our work it ran about 50 times faster than the full R-matrix package. The no-exchange package itself will be published elsewhere (Burke and Burke 1989).

The no-exchange package starts from the requirement that, as in the usual R-matrix method, the $N + 1$ electron Hamiltonian is diagonalised in the basis defined by equation (3). That is we require

$$\langle \psi_k | H_{N+1} | \psi_{k'} \rangle = E_k \delta_{kk'} \tag{5}$$

where the Hamiltonian

$$H_{N+1} = H_N - \tfrac{1}{2}\nabla^2_{N+1} - \frac{Z}{r_{N+1}} + \sum_{\alpha=1}^{N} r^{-1}_{\alpha N+1} \tag{6}$$

and where the integral in equation (5) is carried out over the internal region. For high partial waves, the evaluation of the matrix elements in (5) can be considerably simplified. Firstly, the quadratically integrable functions in equation (3) do not contribute since they are constructed from the bound orbitals whose angular momenta are restricted in our case to $l \le 3$. Secondly, the exchange terms arising from the antisymmetrisation operator in equation (3) are by definition negligible. Hence the only contributions to the Hamiltonian matrix which need to be considered are

$$H_{ijkl} = \langle \bar{\Phi}_i(1, \ldots, N; \hat{r}_{N+1}\sigma_{N+1}) r^{-1}_{N+1} u_k(r_{N+1}) | H_{N+1} |$$
$$\bar{\Phi}_j(1, \ldots, N; \hat{r}_{N+1}\sigma_{N+1}) r^{-1}_{N+1} u_l(r_{N+1}) \rangle. \tag{7}$$

We now summarise the steps in the evaluation of these matrix elements.

Substituting equation (6) into equation (7) yields three terms. The first term is the contribution from the target Hamiltonian H_N which becomes, using an obvious simplified notation,

$$\langle \bar{\Phi}_i r^{-1} u_k(r) | H_N | \bar{\Phi}_j r^{-1} u_l(r) \rangle = E_i \delta_{ij} \delta_{kl} \tag{8}$$

where E_i is the expectation value of the energy in the ith target state. The second term is the contribution from $-\tfrac{1}{2}\nabla^2_{N+1} - Z/r_{N+1}$ which becomes

$$\left\langle \bar{\Phi}_i r^{-1} u_k(r) \left| -\tfrac{1}{2}\nabla^2 - \frac{Z}{r} \right| \bar{\Phi}_j r^{-1} u_l(r) \right\rangle = -\tfrac{1}{2}\delta_{ij} \int_0^a u_k(r) \left(\frac{d^2}{dr^2} - \frac{l_i(l_i+1)}{r^2} + \frac{2Z}{r} \right) u_l(r) \, dr. \tag{9}$$

The final term is the contribution from the electron–electron interaction $\sum_{\alpha=1}^{N} r^{-1}_{\alpha N+1}$ which we write as

$$I_{ijkl} = \left\langle \bar{\Phi}_i r^{-1}_{N+1} u_k(r_{N+1}) \left| \sum_{\alpha=1}^{N} r^{-1}_{\alpha N+1} \right| \bar{\Phi}_j r^{-1}_{N+1} u_l(r_{N+1}) \right\rangle. \tag{10}$$

In order to evaluate I_{ijkl} we expand the electron–electron interaction in the form

$$\sum_{\alpha=1}^{N} r^{-1}_{\alpha N+1} = \sum_{\alpha=1}^{N} \sum_{\lambda=0}^{\infty} \sum_{m=-\lambda}^{\lambda} \frac{r^\lambda_<}{r^{\lambda+1}_>} C^{[\lambda]}_m(r_\alpha) C^{[\lambda]*}_m(\hat{r}_{N+1}) \tag{11}$$

where we have introduced the irreducible tensor operator $C^{[\lambda]}_m$ defined by Fano and Racah (1959). We also use the following expansion of the channel functions $\bar{\Phi}_i$

$$\bar{\Phi}_i(1, \ldots, N; \hat{r}_{N+1}\sigma_{N+1})$$
$$= \sum_{\substack{M_{L_i} m_{l_i} \\ M_{S_i} m_i}} (L_i l_i M_{L_i} m_{l_i} | L M_L)$$
$$\times (S_i \tfrac{1}{2} M_{S_i} m_i | S M_S) \Phi_i(1, \ldots, N) \mathcal{Y}_{l_i m_{l_i}}(\hat{r}_{N+1}) \chi_{\frac{1}{2} m_i}(\sigma_{N+1}) \tag{12}$$

where Φ_i are the target states, $\mathcal{Y}_{l_i m_{l_i}}$ are spherical harmonics defined by Fano and Racah, $\chi_{\frac{1}{2} m_i}$ are electron spin functions and the quantities $(a\,b\,cd | ef)$ are the usual Clebsch–Gordan coefficients. The integral in I_{ijkl} involving the target states Φ_i can

then be written as

$$\left\langle \Phi_i(1,\ldots,N) \left| \sum_{\alpha=1}^{N} \frac{r_<^\lambda}{r_>^{\lambda+1}} C_m^{[\lambda]}(r_\alpha) \right| \Phi_j(1,\ldots,N) \right\rangle$$

$$= \delta_{S_iS_j}\delta_{M_{S_i}M_{S_j}}(2L_i+1)^{-1/2}(L_j\lambda M_{L_j}m|L_iM_{L_i})\sum_{i'j'} c_{i'i}c_{j'j}$$

$$\times \left\langle \alpha_{i'}L_iS_i \left\| \sum_{\alpha=1}^{N} \frac{r_<^\lambda}{r_>^{\lambda+1}} C^{[\lambda]}(\alpha) \right\| \alpha_{j'}L_jS_j \right\rangle \tag{13}$$

where we have used the CI expansion of the target states Φ_i given by equation (2). The reduced matrix element in equation (13) is evaluated using the program TENSOR written by Robb (1973) which calculates the reduced matrix elements of one-particle tensor operators. We find that

$$\left\langle \alpha_{i'}L_iS_i \left\| \sum_{\alpha=1}^{N} \frac{r_<^\lambda}{r_>^{\lambda+1}} C^{[\lambda]}(\alpha) \right\| \alpha_{j'}L_jS_j \right\rangle$$

$$= \sum_{\rho\sigma} V_{i'j'}(\rho\sigma\lambda)\langle\lambda_\rho\|C^{[\lambda]}\|\lambda_\sigma\rangle y_\lambda(n_\rho l_\rho n_\sigma l_\sigma; r_{N+1}) \tag{14}$$

where we sum over the interacting shells ρ and σ in the target configurations and where $V_{ij}(\rho\sigma\lambda)$ is the vector VSHELL defined by Robb (1973) which is output from TENSOR. Collecting up terms and carrying out the integral over r_{N+1} and the summations over the magnetic quantum numbers then yields

$$I_{ijkl} = \delta_{S_iS_j}(-1)^{L_i-L-(l_i+l_j)/2}(2l_i+1)^{1/2}\sum_\lambda (-1)^{\lambda/2}(l_i\lambda 00|l_j0)\,W(L_iL_jl_il_j;\lambda L)$$

$$\times \sum_{i'j'} c_{i'i}c_{j'j}\sum_{\rho\sigma} V_{i'j'}(\rho\sigma\lambda)\langle l_\rho\|C^{[\lambda]}\|l_\sigma\rangle R_\lambda(n_\rho l_\rho n_k l_k; n_\sigma l_\sigma n_l l_l) \tag{15}$$

where the one-electron reduced matrix elements

$$\langle l_\rho\|C^{[\lambda]}\|l_\sigma\rangle = (-1)^{(l_\sigma-l_\rho+\lambda)/2}(2l_\sigma+1)^{1/2}(l_\sigma\lambda 00|l_\rho0). \tag{16}$$

The $W(abcd;ef)$ are Racah coefficients and R_λ are the usual Slater R_λ radial integrals over the four radial wavefunctions. These radial integrals are of course carried out over the internal region $0 \leq r \leq a$.

The Hamiltonian matrix elements in the no-exchange approximation are obtained by summing the contributions defined by equations (8), (9) and (15). The remainder of the calculation then proceeds as in the usual full-exchange calculation described by Burke and Robb (1975) and Berrington *et al* (1974, 1978) using a new asymptotic package written by Seaton (1989). However, we note that because the no-exchange Hamiltonian matrix contains the factor $\delta_{S_iS_j}$ then the problem for high partial waves reduces to solving independent sets of equations for the seven singlet target states and for the five triplet target states. This reduced the size of the Hamiltonian matrices which need to be considered so that as well as calculating the matrix elements very much more rapidly the new no-exchange package also diagonalises these matrices and solves the coupled equations in the asymptotic region more speedily.

4. Convergence of the total collision strength with angular momentum

Collision strengths for the optically allowed transitions were 'topped-up' at large values of the total angular momentum using the sum rule of Burgess (1974) described by

Burke and Seaton (1986). This sum rule can be applied when the Coulomb–Bethe approximation becomes valid. A necessary condition for this is that the point of inflection r should be large compared with the mean radii of the target states r_i where

$$r = \{[Z^2 + \varepsilon_i l_i (l_i + 1)]^{1/2} - Z\}/\varepsilon_i \text{(au)}. \tag{17}$$

Here ε_i and l_i are the energy in Rydbergs and the angular momentum respectively of the electron in channel i and Z is the charge on the target ion.

Figure 1 is a plot of l against ε for different values of r using equation (17). $r = 8$ au corresponds to the radius at which the $n = 2$ orbitals become negligible and $r = 14$ au that at which the $n = 3$ orbitals become negligible. The variation of l with ε becomes steeper as r increases so that at rather high channel energies the l at which the top-up procedure can be applied to collision strengths between $n = 3$ states is larger than that for $n = 2$ states.
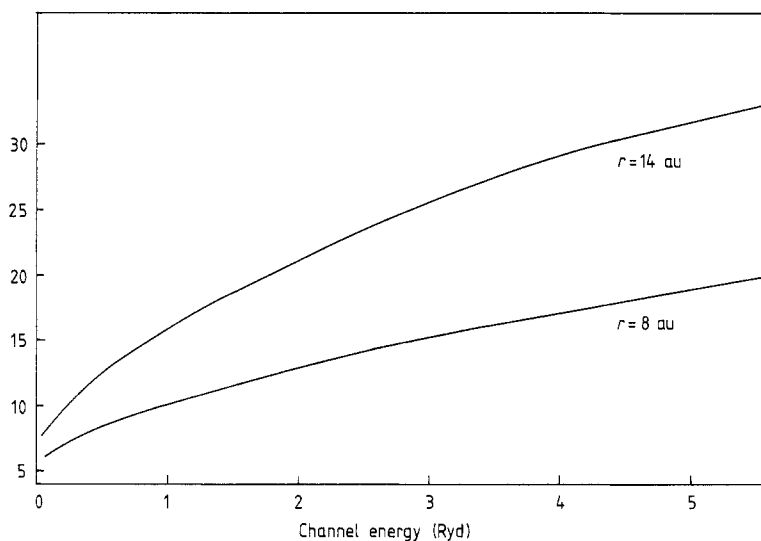

Figure 1. The top-up angular momentum l as a function of channel energy in Rydbergs for $n = 2$ transitions (radius 8 au) and $n = 3$ transitions (radius 14 au).

Near threshold we see that the top-up procedure can be applied at $l \approx 6$–8 for all transitions. However, at the highest energy considered, corresponding to a channel energy of 8 Rydbergs relative to the $2s^2\ {}^1S^e$ state and 5.5 Rydbergs relative to the $2s3d\ {}^3D^e$ state, a top-up at $l = 23$ is necessary for the $n = 2$ transitions and a top-up at $l = 33$ is necessary for the $n = 3$ transitions. Using the Burgess sum rule before the Coulomb–Bethe approximation becomes valid will give incorrect results. As an example at a channel energy of 5.6 Rydbergs the total collision strength for the $2s3p\ {}^3P^o$ to $2s3d\ {}^3D^e$ transition converges to a value of 410 using a top-up at $l = 33$. The value obtained when topping up at $l = 20$ is 510 and at $l = 15$ it is 660.

A top-up procedure was not used for quadrupole transitions such as $2s3d\ {}^3S^e$ to $2s3d\ {}^3D^e$ since these converge by $l = 35$ at the highest energies considered.

Exchange effects were found to be negligible by total angular momentum $L = 10$ where collision strengths calculated using the no-exchange R-matrix code agreed with those calculated using the full R-matrix code within 4%. Hence it was necessary to use the no-exchange code from $L = 11$ to $L \approx 35$ at the highest energies considered.

5. Results

We have calculated effective collision strengths γ_{ij} for all transitions between the six $n = 2$ states and the six $n = 3$ states and for all transitions involving pairs of $n = 3$ states. The effective collision strengths γ_{ij} are related to the collision rates c_{ij} by the expression

$$c_{ij}(\text{cm}^3 \text{ s}^{-1}) = \frac{8.63 \times 10^{-6}}{g_i T_e^{1/2}} \gamma_{ij} \exp(-E_{ij}/kT_e) \tag{18}$$

where T_e is the electron temperature in K, g_i is the statistical weight of the initial state, k is the Boltzmann constant and E_{ij} is the energy difference between the two levels. The main calculations were carried out on the CRAY X-MP/48 at the Atlas Supercomputer Centre and the results analysed on the VAX 11/750 in the School of Mathematics and Physics at Queen's University.

For total angular momenta $L \leq 6$, pseudo-resonances occurred in the energy range between the highest excitation threshold and about 10 Rydbergs. These were due to the inclusion of the quadratically integrable functions χ_j in expansion (3). In order to obtain physically meaningful cross sections and hence effective collision strengths we energy averaged the corresponding T-matrix elements. It was shown by Burke *et al* (1981) that this averaging procedure approximately allows for channels omitted from the calculation. For total angular momenta $L > 6$, pseudo-resonances do not arise and hence energy averaging is not necessary. For the spin-allowed transitions converged cross sections were obtained using the no-exchange package combined with the Burgess sum rule as described in the previous section. As an example of our results we show in figure 2 the collision strength for the $2s^2\ {}^1S^e$–$2s3d\ {}^1D^e$ transition. In order to obtain effective collision strengths over the temperature range from 10^4 to $10^{5.8}$ K total collision strengths up to 8 Rydbergs were determined. Above 8 Rydbergs the total collision strength was extrapolated using an inverse power series in the incident energy E and including a log E term for the dipole allowed transitions (Berrington *et al* 1985).
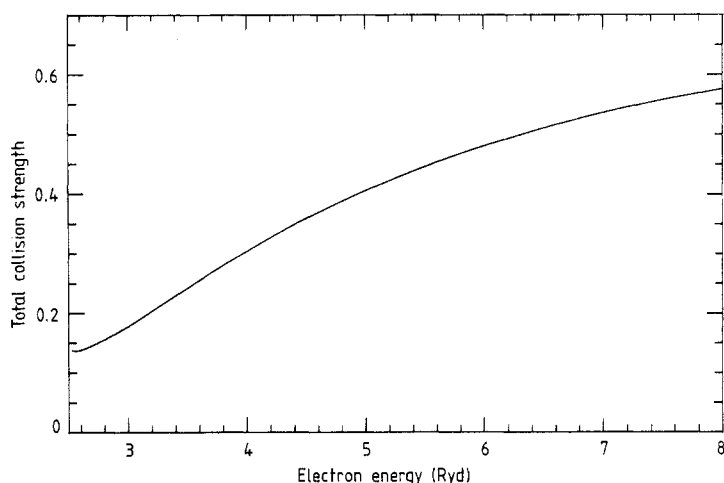
Figure 2. The collision strength for the $2s^2\ {}^1S^e$–$2s3d\ {}^1D^e$ transition over the incident electron energy from threshold to 8 Rydbergs.

Table 3. Effective collision strengths for transitions between the first twelve states of C III for temperature T in the range 10^4 to $10^{5.8}$ K

Transitions		Electron temperature ($\log T$)									
		4.0	4.2	4.4	4.6	4.8	5.0	5.2	5.4	5.6	5.8
1-7	$^1S^e$–$^3S^e$	0.265	0.238	0.203	0.165	0.130	0.100	0.766×10^{-1}	0.588×10^{-1}	0.452×10^{-1}	0.345×10^{-1}
1-8	$^1S^e$–$^1S^e$	0.324	0.307	0.290	0.272	0.256	0.250	0.256	0.273	0.297	0.324
1-9	$^1S^e$–$^1P^o$	0.166	0.156	0.138	0.118	0.102	0.936×10^{-1}	0.949×10^{-1}	0.107	0.132	0.172
1-10	$^1S^e$–$^3P^o$	0.162	0.144	0.123	0.102	0.841×10^{-1}	0.716×10^{-1}	0.633×10^{-1}	0.567×10^{-1}	0.500×10^{-1}	0.423×10^{-1}
1-11	$^1S^e$–$^3D^e$	0.225	0.210	0.196	0.185	0.176	0.167	0.154	0.137	0.117	0.964×10^{-1}
1-12	$^1S^e$–$^1D^e$	0.168	0.161	0.160	0.165	0.177	0.201	0.239	0.292	0.356	0.427
2-7	$^3P^o$–$^3S^e$	3.81	3.21	2.60	2.03	1.55	1.21	1.01	0.915	0.921	1.01
2-8	$^3P^o$–$^1S^e$	0.790	0.723	0.614	0.500	0.402	0.331	0.280	0.237	0.196	0.154
2-9	$^3P^o$–$^1P^o$	0.944	0.868	0.756	0.636	0.529	0.441	0.366	0.302	0.244	0.192
2-10	$^3P^o$–$^3P^o$	4.81	4.38	3.92	3.52	3.21	2.99	2.87	2.84	2.87	2.94
2-11	$^3P^o$–$^3D^e$	4.84	4.69	4.60	4.64	4.85	5.26	5.90	6.84	8.13	9.83
2-12	$^3P^o$–$^1D^e$	0.746	0.693	0.639	0.589	0.539	0.483	0.421	0.356	0.289	0.226
3-7	$^1P^o$–$^3S^e$	1.26	1.07	0.879	0.686	0.516	0.378	0.274	0.198	0.142	0.102
3-8	$^1P^o$–$^1S^e$	0.660	0.601	0.511	0.413	0.327	0.261	0.218	0.195	0.189	0.199
3-9	$^1P^o$–$^1P^o$	1.25	1.16	1.01	0.868	0.755	0.684	0.650	0.642	0.654	0.678
3-10	$^1P^o$–$^3P^o$	1.00	0.936	0.833	0.714	0.601	0.503	0.419	0.345	0.277	0.216
3-11	$^1P^o$–$^3D^e$	1.25	1.12	0.995	0.888	0.794	0.702	0.605	0.508	0.413	0.324
3-12	$^1P^o$–$^1D^e$	1.61	1.64	1.71	1.86	2.10	2.44	2.90	3.50	4.25	5.18
4-7	$^3P^e$–$^3S^e$	0.673	0.641	0.569	0.470	0.366	0.272	0.196	0.138	0.963×10^{-1}	0.672×10^{-1}
4-8	$^3P^e$–$^1S^e$	0.987×10^{-1}	0.934×10^{-1}	0.812×10^{-1}	0.652×10^{-1}	0.499×10^{-1}	0.373×10^{-1}	0.276×10^{-1}	0.202×10^{-1}	0.147×10^{-1}	0.111×10^{-1}
4-9	$^3P^e$–$^1P^o$	1.05	0.946	0.798	0.634	0.482	0.355	0.256	0.182	0.127	0.875×10^{-1}
4-10	$^3P^e$–$^3P^o$	4.79	4.13	3.37	2.63	1.99	1.48	1.10	0.824	0.615	0.456
4-11	$^3P^e$–$^3D^e$	3.97	3.51	2.95	2.38	1.86	1.43	1.08	0.811	0.606	0.450
4-12	$^3P^e$–$^1D^e$	1.30	1.11	0.905	0.717	0.559	0.431	0.328	0.246	0.181	0.131
5-7	$^1D^e$–$^3S^e$	1.50	1.23	0.984	0.760	0.563	0.401	0.278	0.188	0.126	0.835×10^{-1}
5-8	$^1D^e$–$^1S^e$	0.622	0.555	0.460	0.361	0.276	0.211	0.168	0.142	0.129	0.125

Table 3. (continued)

Transitions		Electron temperature ($\log T$)									
		4.0	4.2	4.4	4.6	4.8	5.0	5.2	5.4	5.6	5.8
5–9	$^1D^e$–$^1P^o$	1.66	1.57	1.40	1.21	1.05	0.953	0.927	0.966	1.06	1.19
5–10	$^1D^e$–$^3P^o$	1.99	1.93	1.70	1.37	1.05	0.762	0.540	0.376	0.259	0.176
5–11	$^1D^e$–$^3D^e$	2.42	2.11	1.73	1.35	1.02	0.747	0.540	0.388	0.277	0.195
5–12	$^1D^e$–$^1D^e$	1.39	1.24	1.08	0.952	0.851	0.773	0.712	0.666	0.637	0.619
6–7	$^1S^e$–$^3S^e$	0.519	0.469	0.392	0.308	0.230	0.165	0.116	0.812×10^{-1}	0.562×10^{-1}	0.384×10^{-1}
6–8	$^1S^e$–$^1S^e$	0.471	0.428	0.364	0.296	0.236	0.186	0.149	0.122	0.103	0.928×10^{-1}
6–9	$^1S^e$–$^1P^o$	0.219	0.222	0.212	0.195	0.177	0.164	0.160	0.167	0.185	0.214
6–10	$^1S^e$–$^3P^o$	0.262	0.253	0.222	0.181	0.141	0.108	0.807×10^{-1}	0.598×10^{-1}	0.436×10^{-1}	0.312×10^{-1}
6–11	$^1S^e$–$^3D^e$	0.272	0.256	0.230	0.199	0.166	0.135	0.107	0.828×10^{-1}	0.625×10^{-1}	0.461×10^{-1}
6–12	$^1S^e$–$^1D^e$	0.438	0.396	0.353	0.317	0.292	0.279	0.277	0.282	0.289	0.295
7–8	$^3S^e$–$^1S^e$	3.46	2.87	2.26	1.71	1.26	0.915	0.669	0.489	0.357	0.257
7–9	$^3S^e$–$^1P^o$	2.41	1.93	1.49	1.13	0.854	0.650	0.496	0.376	0.281	0.206
7–10	$^3S^e$–$^3P^o$	62.5	65.7	63.8	62.8	66.9	76.2	89.3	105.3	123.0	141.7
7–11	$^3S^e$–$^3D^e$	9.81	10.1	10.4	10.8	11.3	11.9	12.6	13.3	13.8	14.2
7–12	$^3S^e$–$^1D^e$	0.794	0.747	0.695	0.641	0.582	0.517	0.442	0.363	0.286	0.215
8–9	$^1S^e$–$^1P^o$	13.5	14.0	14.9	17.0	20.6	25.6	31.5	38.0	44.6	51.0
8–10	$^1S^e$–$^3P^o$	2.12	1.76	1.40	1.08	0.821	0.624	0.475	0.358	0.266	0.192
8–11	$^1S^e$–$^3D^e$	1.62	1.37	1.14	0.941	0.766	0.616	0.488	0.377	0.283	0.206
8–12	$^1S^e$–$^1D^e$	3.03	3.07	3.18	3.37	3.62	3.89	4.15	4.38	4.55	4.64
9–10	$^1P^o$–$^3P^o$	9.56	8.15	6.60	5.16	3.97	3.03	2.32	1.76	1.32	0.966
9–11	$^1P^o$–$^3D^e$	3.99	3.43	2.92	2.50	2.14	1.81	1.50	1.19	0.909	0.667
9–12	$^1P^o$–$^1D^e$	32.4	33.4	35.7	39.6	45.1	52.0	60.3	69.6	80.0	91.8
10–11	$^3P^o$–$^3D^e$	98.1	103.9	114.9	133.6	159.7	191.0	225.6	262.4	301.3	344.7
10–12	$^3P^o$–$^1D^e$	2.77	2.63	2.48	2.32	2.12	1.87	1.58	1.27	0.967	0.708
11–12	$^3D^e$–$^1D^e$	9.06	8.58	8.05	7.46	6.76	5.91	4.95	3.96	3.04	2.25

For the temperatures of importance in this paper the contribution from energies above 8 Rydbergs is small and this extrapolation gave negligible error.

Our final effective collision strengths for temperatures in the range 10^4 to $10^{5.8}$ K are presented in table 3. The levels in this table are labelled from 1 to 12 in order of increasing energy defined in table 2.

6. Conclusions

In this paper we have described our latest calculations of effective collision strengths involving the six states of the $2s3l$ configurations in C III. These calculations have provided the most accurate data currently available for these states and they have already been used in the analysis of radiation from JET (H P Summers, private communication). The next step in our work on C III is to include also the fourteen states of the $2p3l$ configurations in the collision expansion. This is a much larger calculation, but our new no-exchange package combined with the power of the CRAY X-MP/48 make such a study now feasible.

Acknowledgments

References

Berrington K A 1985 *J. Phys. B: At. Mol. Phys.* **18** L395
Berrington K A, Burke P G, Chang J J, Chivers A J, Robb W D and Taylor K T 1974 *Comput. Phys. Commun.* **8** 149
Berrington K A, Burke P G, Dufton P L and Kingston A E 1977 *J. Phys. B: At. Mol. Phys.* **10** 1465
—— 1981 *At. Data Nucl. Data Tables* **26** 1
—— 1985 *At. Data Nucl. Data Tables* **33** 195
Berrington K A, Burke P G, Le Dourneuf M, Robb W D, Taylor K T and Vo Ky Lan 1978 *Comput. Phys. Commun.* **14** 367
Burgess A 1974 *J. Phys. B: At. Mol. Phys.* **7** L364
Burke P G, Berrington K A and Sukumar C V 1981 *J. Phys. B: At. Mol. Phys.* **14** 287
Burke P G and Burke V M 1989 *Comput. Phys. Commun.* to be submitted.
Burke P G, Hibbert A and Robb W D 1972 *J. Phys. B: At. Mol. Phys.* **5** 37
Burke P G and Robb W D 1975 *Adv. At. Mol. Phys.* **11** 143
Burke V M and Seaton M J 1986 *J. Phys. B: At. Mol. Phys.* **19** L527
Dufton P L, Berrington K A, Burke P G and Kingston A E 1978 *Astron. Astrophys.* **62** 111
Dufton P L and Kingston A E 1981 *Adv. At. Mol. Phys.* **17** 355
Doyle J G and McWhirter R W P 1980 *Mon. Not. R. Astron Soc.* **193** 947
Fano U and Racah G 1959 *Irreducible Tensorial Sets* (New York: Academic)
Gabriel A H and Jordan C 1972 *Case Studies in Atomic Collision Physics* vol 2, ed E W McDaniel and M R C McDowell (Amsterdam: North-Holland) p 209
Glass R 1979 *J. Phys. B: At. Mol. Phys.* **12** 1633
Hibbert A 1975 *Comput. Phys. Commun.* **9** 141
—— 1976 *J. Phys. B: At. Mol. Phys.* **9** 2805

Keenan F P, Berrington K A, Burke P G, Dufton P L and Kingston A E 1984 *Mon. Not. R. Astron. Soc.* **207** 459

Moore C E 1970 *NSRDS-NBS 3* (Washington DC: National Bureau of Standards) § 3

Robb W D 1973 *Comput. Phys. Commun.* **6** 132

Seaton M J 1989 *Comput. Phys. Commun.* to be submitted

Yu Yan and Seaton M J 1987a *J. Phys. B: At. Mol. Phys.* **20** 6409

—— 1987b *J. Phys. B: At. Mol. Phys.* **20** 6431

Yu Yan, Taylor K T and Seaton M J 1987 *J. Phys. B: At. Mol. Phys.* **20** 6399